American Mineralogist, Volume 91, pages 1323–1330, 2006

Light-induced changes in molecular arsenic sulfides: State of the art and new evidence by single-crystal X-ray diffraction

PAOLA BONAZZI,* LUCA BINDI, GIOVANNI PRATESI, AND SILVIO MENCHETTI

Dipartimento di Scienze della Terra, Università di Firenze, via La Pira 4, I-50121 Firenze, Italy

ABSTRACT

Light-induced structural changes in single crystals belonging to the β-As_4S_4-As_8S_9 series and in a crystal of synthetic β-As_4S_3 were monitored step by step by determining the unit-cell dimensions. A marked increase of unit-cell volume as a function of exposure time was observed for all the crystals belonging to the β-As_4S_4-As_8S_9 series except for stoichiometric alacranite (As_8S_9). No significant change upon long exposures to light was observed for the synthetic β-As_4S_3 crystal. Crystal structure refinements were carried out for crystals with different composition at selected steps of the light-induced process. The structural results clearly showed that the percentage of the As_4S_5 molecule in the structure increases when a crystal is exposed to light. Therefore, the increment of the unit-cell volume induced by light exposure appears to be related to a random replacement of As_4S_5 for As_4S_4 in the structure according to the reaction $5As_4S_4 + 3O_2 \rightarrow 4As_4S_5 + 2As_2O_3$. The results obtained in the present study combined with a critical review of data previously published indicate that the As_4S_4 molecule is able to incorporate sulfur to convert to As_4S_5 upon exposure to light, whereas either As_4S_3 or As_4S_5 molecules do not go undergo any modification. It appears that the extent of sulfur incorporation is strictly controlled by the type of molecular packing as well as by the kind of molecule.

A final, complete conversion to pararealgar was observed only for pure β-As_4S_4, whereas non-stoichiometric As_8S_{9-x} crystals initially containing variable amounts of β-As_4S_4 microdomains convert only partially to pararealgar upon light exposure.

Keywords: XRD data, arsenic sulfides, crystal structure, light-induced alteration, alacranite, β-As_4S_4

INTRODUCTION

Most of the arsenic sulfides have a crystal structure consisting of a packing of cage-like, covalently bonded As_4S_n ($n = 3$, 4, and 5) molecules held together by van der Waals forces. Four types of As_4S_n molecular units are known. Both the α-dimorphite ($T < \sim 70$ °C) (Whitfield 1973a) and β-dimorphite ($T > \sim 70$ °C) (Whitfield 1970) structures are based on the same As_4S_3 molecule. Realgar (Mullen and Nowacki 1972) and the high-temperature polymorph β-As_4S_4 (Porter and Sheldrick 1972) consist of a packing of the same As_4S_4 molecule, which, however, is different from the As_4S_4 molecule found in pararealgar (Bonazzi et al. 1995) and in the synthetic As_4S_4(II) synthesized by Kutoglu (1976). The structure of uzonite is based on a packing of As_4S_5 molecules (Whitfield 1973b; Bindi et al. 2003) whereas the structure of alacranite (Bonazzi et al. 2003a), As_8S_9, consists of an ordered packing of As_4S_4 and As_4S_5, with a molecular arrangement closely resembling that found in the β-As_4S_4. The coexistence of both As_4S_4 and As_4S_5 molecules was also found in the non-stoichiometric sulfide minerals from Kateřina mine (Bonazzi et al. 2003b), which have chemical compositions ranging continuously from As_8S_8 to As_8S_9. Finally, cage-like As_4S_5 molecular units were also found in the structure of wakabayashilite, $[(As,Sb)_6S_9][As_4S_5]$ (Bonazzi et al. 2005). It is noteworthy that the As_4S_6 cage-like molecule has never been found in arsenic sulfides: orpiment, which has atomic ratio As:S = 4:6, exhibits a layered structural arrangement (Mullen and Nowacki 1972).

It has been long known that exposure of realgar to light induces its alteration at the surface into friable, yellow films consisting of pararealgar (Roberts et al. 1980). Whenever the rate of the process is lowered, by using opportune filters (550 nm long-wavelength pass filter), light alters both realgar and β-phase up to pararealgar through an intermediate product called χ-phase (Douglass et al. 1992; Bonazzi et al. 1996; Muniz-Miranda et al. 1996). The initial steps of the light-induced process occur with a strong increase of the unit-cell volume in both realgar and β-As_4S_4 (Bonazzi et al. 1996). However, the process starting from realgar is discontinuous and it can be monitored on altered single crystals only during the first steps of alteration (Bonazzi et al. 1996). On the contrary, the process leading to the formation of the χ-phase from the β-phase can be monitored step by step following the powder diffraction pattern as well as the Raman spectrum, which change continuously until they approach eventually those of the χ-phase. Thus, the χ-phase was considered as an expanded, less-ordered β-phase (Bonazzi et al. 1996), probably characterized by a lower molecular symmetry (Muniz-Miranda et al. 1996). Because the β-phase structure transforms gradually into that of the χ-phase, it appeared sensible to us to investigate the light-induced structural changes starting from β-phase rather than from realgar single-crystals. Thus, the intensity data were collected for a synthetic β-As_4S_4 crystal (unpublished data) at

* E-mail: pbcry@geo.unifi.it

different steps of the light treatment.

Later, the microchemical and structural study of non-stoichiometric As_8S_{9-x} minerals (Bonazzi et al. 2003b) and of alacranite (Bonazzi et al. 2003a) allowed us to clarify the relationship between the unit-cell volume and the S content along the continuous series existing between the high-temperature polymorph β-As_4S_4 and the mineral alacranite (As_8S_9). The results of these studies indicated that as the percentage of the As_4S_5 molecule increases in the series, the unit-cell volume increases accordingly. To control the variability of the unit-cell parameters with light exposure in minerals containing As_4S_5 molecules alone, crystals of uzonite (Bindi et al. 2003) and wakabayashilite (Bonazzi et al. 2005) were also exposed to light. In these cases, the As_4S_5 molecules remain unchanged, in contrast to the As_4S_4 molecules. It was suggested on this basis (Bindi et al. 2003; Bonazzi et al. 2005) that the increase of the unit-cell volume observed in realgar and β-phase crystals exposed to light could be related to an increase in the percentage of As_4S_5 molecules in the structure according to the following reaction: $5As_4S_4 + 3O_2 \rightarrow 4As_4S_5 + 2As_2O_3$. Indeed, the formation of arsenolite in the light-induced process of alteration of realgar to pararealgar has been reported (Ballirano and Maras 2002).

The hypothesis that oxygen plays an important role in the light-induced alteration of arsenic sulfides was recently supported by X-ray photoelectron spectroscopic measurements of light-exposed realgar reported by Kyono et al. (2005). These authors also report the structural data of a light-exposed crystal of realgar and hypothesize that in the case of realgar the increase of the unit-cell volume is caused by the partial replacement of As_4S_4 molecules by As_4S_5 molecules, although no structural evidence is given to support this hypothesis.

To contribute to the understanding of the effects of light exposure on the arsenic sulfides, further structural data were obtained in this study on different members along the high-temperature polymorph β-As_4S_4-alacranite (As_8S_9) series using single crystal X-ray diffraction methods at different steps of the light-induced process.

Experimental method

Different crystals belonging to the β-As_4S_4-As_8S_9 series and a crystal of synthetic β-As_4S_3 (see Hall 1966 for synthesis method) were exposed to filtered polychromatic light (550 nm long-wavelength pass filter) using the same apparatus described by Bonazzi et al. (1996). After each light exposure, unit-cell parameters were determined by centering 25 relatively strong reflections ($\theta < 14°$) using an Enraf Nonius CAD4 diffractometer until it was still possible to center the same set of reflections. At this stage, crystals were further exposed to light for 24 h and a peak searching routine was repeated. Only in the case of the synthetic β-As_4S_4 (B2; Bonazzi et al. 1996) was it possible to determine the unit-cell parameters that were found to correspond to those of pararealgar. The crystals were then mounted (exposure time of 100 s per frame; 40 mA × 40 kV) on a CCD-equipped diffractometer (Oxford Xcalibur 2). B2 crystal did not reveal any peaks other than those belonging to the pararealgar structure [determined unit-cell parameters were: a = 9.91(2), b = 9.655(9), c = 8.526(9) Å, and β = 96.8(1)°]. The other crystals exhibited weak and broad peaks, which were not consistent with an unique phase. Only in the case of ALA16 and ALA15 it was possible to index a fraction of the collected reflections (80 and 55%, respectively) with the unit cell of pararealgar. All the crystals examined did not exhibit any peaks belonging to the arsenolite phase.

Table 1 reports the unit-cell parameters vs. increasing light-exposure times for the non-stoichiometric As_8S_{9-x} crystals ALA16, ALA15, and ALA2 from the Kateřina Mine, Czech Republic (Bonazzi et al. 2003b) and for alacranite ALA-TL from the type locality (Bonazzi et al. 2003a). The unit-cell parameters of the synthetic β-As_4S_3 crystal [a = 9.159(1), b = 8.033(1), and c = 10.199(2) Å for the untreated crystal] did not exhibit any significant change upon long exposures to light (the shifts were within the standard deviations).

Intensity data were collected at selected steps of the light-induced process for ALA16 and ALA15 crystals. Experimental details are reported in Table 2 together with those of the data collections previously carried out for the synthetic β-As_4S_4 (B2 crystal; unit-cell dimensions measured after light-exposure times up to 1860 min are reported in Bonazzi et al. 1996). The hkl reflections having $h + k$ = 2n +1 and $h0l$ reflections having l = 2n + 1 were systematically absent for all the data collections. Therefore, the space group $C2/c$ previously determined for the β-As_4S_4 phase (Porter and Sheldrick 1972) and for the untreated non-stoichiometric As_8S_{9-x} crystals (Bonazzi et al. 2003b) was confirmed. Nonetheless, weak reflections violating the C symmetry were observed for all the crystals examined except for B2-0. The intensity of the most evident violations (i.e., 5 0 0, $\bar{3}$ 2 1, $\bar{6}$ 1 1, 3 2 2, $\bar{1}$ 4 2, 3 0 4) was measured at different steps of the light exposure. Intensities were treated for Lorentz-polarization effects and subsequently corrected for absorption following the semi-empirical method of North et al. (1968). Monoclinic-equivalent reflections were averaged.

Structure refinements

For the untreated, synthetic β-As_4S_4 crystal (B2-0) the $C2/c$ structure of the synthetic β-As_4S_4 phase was assumed as starting model. Structure refinement was performed on F^2 using the SHELXL-97 program (Sheldrick 1997). Convergence was quickly achieved for an anisotropic model to R_{obs} = 2.80%. However, after variable exposure to light (B2-600 and B2-840 data sets) the structural refinement was not as straight forward. Isotropic full-matrix least-squares cycles were initially run assuming the atom sites were fully occupied, although the unusually high value of the isotropic displacement factor for the S2 atom strongly suggested partial occupancy at this site. As in the case of non-stoichiometric As_8S_{9-x} crystals (Bonazzi et al. 2003b), an examination of the ΔF-Fourier map revealed the presence of residual peaks clearly indicating split positions for both As atoms (As1b and As2b) and an additional position for a S atom (S4). The convergence was quickly achieved by adding these peaks to the atom array without applying constraints to their occupancy factors. For both B2-600 and B2-840, the occupancy factors of As1, As2, and S2 refined close to a common value (k), while the occupancy factors of As1b, As2b, and S4 were approximately equal to 1-k. S1 and S3 appeared to be fully occupied. The simultaneous coexistence of As1b + As2b with S2 and of As1 + As2 with S4 was excluded on the basis of the bond distances. Therefore, we adopted the same strategy as that used to refine the structure of the untreated, non-stoichiometric As_8S_{9-x} crystals (Bonazzi et al. 2003b): i.e., to reduce the number of free variables and obtain a reliable model, only one parameter (k) was refined to constrain occ.(As1) = occ.(As2) = occ.(S2) = k, and occ.(As1b) = occ.(As2b) = occ.(S4) = 1-k. Successive cycles were run with an anisotropic model. The value of (1-k), which is a measure of the fraction of the As_4S_5 molecule substituting for As_4S_4, was found to be 0.17(1) and 0.22(1) for B2-600 and B2-840, respectively.

The structure refinements ALA16-0 and ALA16-1800, which was carried out using the same procedure, led to similar models, with (1-k) = 0.131(6) and 0.31(1), before and after the light exposure, respectively. Finally, with the ALA15 structure as a starting model (Bonazzi et al. 2003b), convergence was quickly obtained for ALA15-600. The value (1-k), which was 0.21(1) in the untreated crystal, was found to be 0.38(2) after exposure. Atomic coordinates and anisotropic displacement parameters are reported in Table 3.

TABLE 1. Unit-cell parameters of arsenic sulfides measured after different light-exposure times

t (min)	*a* (Å)	*b* (Å)	*c* (Å)	β (°)	*V* (Å³)
ALA16					
0*	9.963(3)	9.323(3)	8.962(4)	102.41(3)	813.0(1)
150	9.955(3)	9.334(3)	8.951(6)	102.20(8)	812.9(6)
300	9.950(3)	9.347(3)	8.952(6)	102.01(8)	814.3(6)
450	9.949(3)	9.360(3)	8.963(5)	101.83(4)	816.9(5)
600	9.943(3)	9.370(3)	8.968(5)	101.76(4)	818.0(5)
750	9.933(3)	9.379(2)	8.972(5)	101.75(4)	818.3(5)
900	9.923(3)	9.385(3)	8.985(5)	101.63(4)	819.6(5)
1050	9.922(3)	9.389(2)	8.997(4)	101.62(3)	821.0(4)
1200	9.919(3)	9.397(2)	9.010(4)	101.54(3)	822.8(4)
1350	9.887(3)	9.422(3)	9.044(3)	101.54(2)	825.5(4)
1500	9.881(3)	9.425(3)	9.051(3)	101.45(3)	826.1(4)
1650	9.875(3)	9.427(3)	9.060(3)	101.43(3)	826.7(4)
1800*	9.862(3)	9.438(3)	9.078(4)	101.25(3)	828.7(4)
1950	9.849(3)	9.448(3)	9.086(3)	101.32(3)	829.0(4)
2100	9.850(4)	9.449(2)	9.090(3)	101.18(3)	830.0(4)
2250	9.846(4)	9.451(3)	9.098(3)	101.18(3)	830.5(4)
2400	9.841(4)	9.457(3)	9.103(4)	101.12(3)	831.3(4)
2550	9.846(4)	9.455(3)	9.099(3)	101.16(3)	831.0(4)
2700	9.837(4)	9.458(3)	9.111(4)	101.07(3)	831.9(4)
2850	9.846(4)	9.454(3)	9.121(3)	101.01(3)	833.4(4)
3000	9.841(5)	9.452(3)	9.128(3)	100.98(3)	833.5(5)
3150	9.842(5)	9.452(5)	9.131(4)	100.94(4)	834.0(5)
3300	9.852(6)	9.441(6)	9.135(5)	100.83(5)	834.5(7)
3450	9.842(6)	9.446(7)	9.128(7)	100.77(6)	833.7(8)
3600	9.839(5)	9.447(7)	9.130(7)	100.71(5)	833.8(8)
3750	9.839(6)	9.450(6)	9.127(9)	100.72(7)	833.8(9)
3900	9.846(7)	9.447(7)	9.120(9)	100.70(7)	833.5(8)
4050	9.849(6)	9.451(8)	9.113(9)	100.69(7)	833.5(8)
4200	9.864(6)	9.438(8)	9.117(9)	100.65(7)	834.1(9)
4500	9.874(9)	9.441(9)	9.108(9)	100.56(9)	835(1)
4800	9.913(9)	9.411(9)	9.111(9)	100.58(9)	836(1)
5100	9.967(9)	9.397(8)	9.095(5)	100.39(6)	837.9(9)
5400	9.978(9)	9.390(8)	9.093(8)	100.31(9)	838(1)
5700	10.01(1)	9.394(9)	9.09(1)	100.3(1)	841(1)
6000	9.967(8)	9.41(1)	9.095(6)	100.28(5)	839(2)
6300	9.965(8)	9.42(1)	9.088(9)	100.14(8)	839(2)
ALA15					
0†	9.940(2)	9.398(2)	9.033(2)	102.12(2)	825.0(2)
90	9.924(5)	9.409(1)	9.048(4)	101.92(2)	826.6(5)
180	9.916(6)	9.412(1)	9.060(5)	101.81(3)	827.7(7)
300	9.910(8)	9.423(2)	9.076(6)	101.68(3)	830.0(9)
420	9.895(7)	9.441(2)	9.099(6)	101.46(3)	833.1(8)
540	9.888(7)	9.440(2)	9.106(6)	101.35(3)	834.0(9)
600*	9.885(7)	9.446(2)	9.118(6)	101.32(3)	834.8(8)
720	9.879(8)	9.452(2)	9.128(7)	101.28(3)	835.8(9)
840	9.873(7)	9.455(2)	9.140(6)	101.18(3)	837.0(8)
960	9.866(9)	9.455(2)	9.149(8)	101.13(4)	837.4(9)
1080	9.866(6)	9.453(2)	9.155(5)	101.07(3)	837.9(7)
1200	9.869(7)	9.448(2)	9.160(6)	100.95(3)	838.6(9)
1320	9.877(6)	9.440(2)	9.158(6)	100.90(3)	838.5(8)
1440	9.877(9)	9.434(3)	9.165(8)	100.77(4)	838.9(9)
1560	9.894(9)	9.419(3)	9.160(8)	100.64(4)	839.0(9)
1680	9.91(1)	9.407(4)	9.162(9)	100.51(5)	839(1)
1800	9.93(1)	9.405(4)	9.15(1)	100.53(6)	840(1)
1920	9.94(1)	9.397(3)	9.15(1)	100.51(4)	840(1)
2040	9.96(1)	9.384(4)	9.14(1)	100.24(6)	841(2)
2160	9.98(2)	9.377(4)	9.14(1)	100.15(5)	841(2)
2280	9.99(2)	9.381(4)	9.13(1)	100.21(5)	842(2)
2400	9.99(2)	9.368(4)	9.13(1)	100.04(6)	842(2)
2520	10.00(2)	9.374(4)	9.12(1)	100.12(6)	842(2)
2640	10.01(2)	9.371(4)	9.11(1)	100.05(5)	842(2)
2760	10.00(2)	9.372(4)	9.10(1)	100.07(6)	840(2)
2880	10.01(3)	9.373(5)	9.10(1)	100.00(6)	841(3)
3000	10.03(3)	9.385(5)	9.09(1)	100.09(6)	842(2)
3120	10.04(1)	9.382(4)	9.09(1)	99.95(4)	844(1)
3240	10.06(1)	9.378(6)	9.08(1)	99.93(5)	844(2)
3360	10.05(1)	9.393(5)	9.08(1)	99.94(5)	845(1)
3480	10.06(1)	9.402(6)	9.08(1)	99.94(6)	846(1)
3600	10.06(1)	9.408(8)	9.07(1)	99.85(5)	846(1)
3720	10.06(1)	9.421(9)	9.08(1)	99.83(5)	847(1)
3840	10.06(1)	9.43(1)	9.08(1)	99.80(6)	848(1)
3960	10.06(1)	9.43(1)	9.07(1)	99.77(6)	848(2)
4080	10.07(1)	9.46(3)	9.05(1)	99.77(8)	849(3)
ALA2					
0†	9.936(2)	9.458(2)	9.106(2)	101.90(2)	837.3(3)
90	9.902(8)	9.474(4)	9.134(5)	101.70(5)	839.1(3)
210	9.901(5)	9.492(3)	9.155(3)	101.53(3)	843.0(4)
360	9.901(6)	9.504(6)	9.178(4)	101.33(4)	846.8(4)
480	9.924(6)	9.493(6)	9.186(6)	101.14(5)	849.1(5)
630	9.933(7)	9.486(7)	9.191(8)	101.03(6)	850.0(7)
750	9.962(8)	9.456(8)	9.187(9)	100.78(8)	851.0(6)
1000	9.982(8)	9.438(9)	9.19(1)	100.56(9)	851.0(6)
1150	9.987(6)	9.435(8)	9.19(1)	100.52(7)	851.0(7)
1300	9.991(6)	9.430(7)	9.19(1)	100.47(7)	851.0(8)
1450	9.992(6)	9.426(7)	9.19(1)	100.36(7)	851.0(7)
1600	9.997(6)	9.426(8)	9.19(1)	100.36(7)	852.0(8)
1750	9.999(7)	9.426(7)	9.19(1)	100.32(7)	852.0(8)
1960	10.005(6)	9.424(8)	9.19(1)	100.27(6)	853.0(8)
2170	10.006(5)	9.415(9)	9.19(1)	100.25(7)	852.0(9)
2380	9.997(5)	9.405(8)	9.21(1)	99.87(4)	853(1)
2620	10.005(7)	9.404(8)	9.21(2)	99.9(1)	854(1)
2860	10.01(1)	9.42(2)	9.20(2)	99.8(2)	855(1)
ALA-TL					
0‡	9.942(4)	9.601(2)	9.178(3)	101.94(3)	857.1(5)
240	9.963(5)	9.576(3)	9.197(5)	101.77(3)	859.0(8)
480	9.963(6)	9.573(3)	9.200(6)	101.72(3)	859.1(9)
720	9.966(6)	9.572(3)	9.194(5)	101.69(3)	858.9(8)
960	9.961(7)	9.570(4)	9.198(7)	101.69(3)	858.6(9)
1200	9.962(7)	9.571(4)	9.195(7)	101.68(3)	858.6(9)
1440	9.965(6)	9.570(3)	9.199(5)	101.71(3)	859.0(8)

* Intensity data collection was performed at this stage. All the unit-cell parameters and their standard deviations (reported in parentheses) were determined using an Enraf Nonius CAD4 diffractometer with the SETANG routine iteratively combined with the least squares method and refined with constrains by the CELDIM routine.
† Structural data of the untreated ALA15 and ALA2 crystals are reported in Bonazzi et al. (2003b).
‡ Structural data for alacranite (ALA-TL) is reported in Bonazzi et al. (2003a).

RESULTS

A marked increase of the unit-cell volume as a function of the exposure time (Fig. 1) was observed for all the crystals (B2, ALA16, ALA15, ALA2) except for ALA-TL, where only a minor increment was observed. On the contrary, no significant change upon long exposures to light was observed for the synthetic β-As_4S_3 crystal.

The increase is not monotonous as a function of the exposure time: the trend of increasing unit-cell volume is highest during the first steps of the process, while the rate of change decreased with continued exposure. For crystals with intermediate composition (i.e., ALA16, ALA15, and ALA2), there is a change in the slope of the unit-cell expansion curve (i.e., zero slope) at different values of the unit-cell volume (~834, ~842, and ~851 Å³ for ALA16, ALA15, and ALA2, respectively), which persists for different exposure times. To make the variation of the unit-cell parameters in different crystals comparable, much care was devoted to use the same procedure in the light-exposure experiments; nonetheless, other variables such as the size and the shape of the crystal might affect the alteration rate. Therefore, the unit-cell parameters determined after each light exposure (Table 1) were plotted vs. the unit-cell volume rather than exposure times (Fig. 2). The expansion of the unit cell appears considerably anisotropic. During the first part of the process (hereafter named "path I"), the *a* parameter decreases while *b* and *c* increase. During the subsequent part of the process ("path II"), the *a* parameter

TABLE 2. Experimental details of intensity data collections and structure refinements

	B2-0	B2-600	B2-840
a (Å)	9.958(2)	9.881(3)	9.831(2)
b (Å)	9.311(2)	9.397(5)	9.444(2)
c (Å)	8.867(2)	8.930(2)	8.986(3)
β (°)	102.57(1)	101.64(2)	101.36(2)
V (Å^3)	802.4(3)	812.1(5)	818.0(4)
Z	4	4	4
space group	*C*2/*c*	*C*2/*c*	*C*2/*c*
wavelength	Mo*K*α	Mo*K*α	Mo*K*α
(mA × kV)	(20 × 50)	(20 × 50)	(26 × 50)
2theta-range (°)	2–60	2–60	2–60
crystal size (μm)	225 × 350 × 400	225 × 350 × 400	225 × 350 × 400
scan mode	ω	ω	ω
scan width (°)	2.5	3.0	3.0
variable scan speed (°/min)	2.7–16.5	1.6–16.5	1.1–8.2
index ranges	$-13 \le h \le 13$	$-13 \le h \le 13$	$-13 \le h \le 13$
	$-13 \le h \le 13$	$-13 \le h \le 13$	$-13 \le h \le 13$
	$0 \le l \le 12$	$0 \le l \le 12$	$0 \le l \le 12$
minimum transmission (%)	56.3	57.0	57.4
no. of collected refl.	2420	2421	2493
independent refl.	1174	1176	1194
refl. with $F_o > 4\sigma(F_o)$	834	625	575
R_{obs} (%)	2.80	5.23	7.05
largest diffraction peak and hole (e$^-$/Å^3)	0.92–1.03	2.31–1.19	1.91–0.82
% As_4S_5 molecule	0	17	22

	ALA16-0	ALA16-1800	ALA15-600
a (Å)	9.963(3)	9.862(3)	9.885(7)
b (Å)	9.323(3)	9.438(3)	9.446(2)
c (Å)	8.962(4)	9.078(4)	9.118(6)
β (°)	102.41(3)	101.25(3)	101.32(3)
V (Å^3)	813.0(1)	828.7(4)	834.8(8)
Z	4	4	4
space group	*C*2/*c*	*C*2/*c*	*C*2/*c*
wavelength	Mo*K*α	Mo*K*α	Mo*K*α
(mA × kV)	26 × 50	26 × 50	26 × 50
2theta-range (°)	2–60	2–60	2–58
crystal size (μm)	110 × 165 × 200	110 × 165 × 200	60 × 90 × 110
scan mode	ω	ω	ω
scan width (°)	2.7	3.0	3.0
scan speed (°/min)	3.3	2.1	2.1
index ranges	$-13 \le h \le 13$	$-13 \le h \le 13$	$-12 \le h \le 12$
	$-13 \le h \le 13$	$-13 \le h \le 13$	$-13 \le h \le 12$
	$0 \le l \le 12$	$0 \le l \le 12$	$0 \le l \le 12$
minimum transmission (%)	67.2	68.0	73.4
no. of collected refl.	2411	2443	2119
independent refl.	1141	1157	1002
refl. with $F_o > 4\sigma(F_o)$	713	439	316
R_{obs} (%)	5.11	9.30	9.28
largest diffraction peak and hole (e$^-$/Å^3)	0.84–0.69	0.99–0.68	0.86–0.61
% As_4S_5 molecule	13	31	38

increases while *b* and *c* decrease. However, this inversion of slope is not observed for the end-members of the series (B2 and ALA-TL). The alteration of the stoichiometric β-As_4S_4 crystal (B2) proceeds without inversion following a continuous variation of the *a*, *b*, and *c* parameters according to "path I" alone. On the other hand, the crystal of alacranite (ALA-TL) exhibits only minor variations, which, however, resemble "path II." There is a further trend ("path III") particularly evident for ALA15 and, to a lesser extent, ALA2: the *a* parameter remains almost unchanged, *b* increases again, while *c* still decreases, although with a different, smoother slope. The value of the monoclinic angle β (Fig. 2d) strongly decreases during the entire process for all crystals except for ALA-TL.

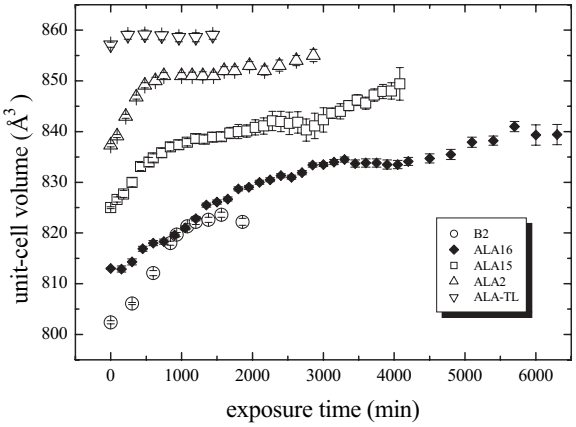

FIGURE 1. Variation of unit-cell volume as a function of exposure time.

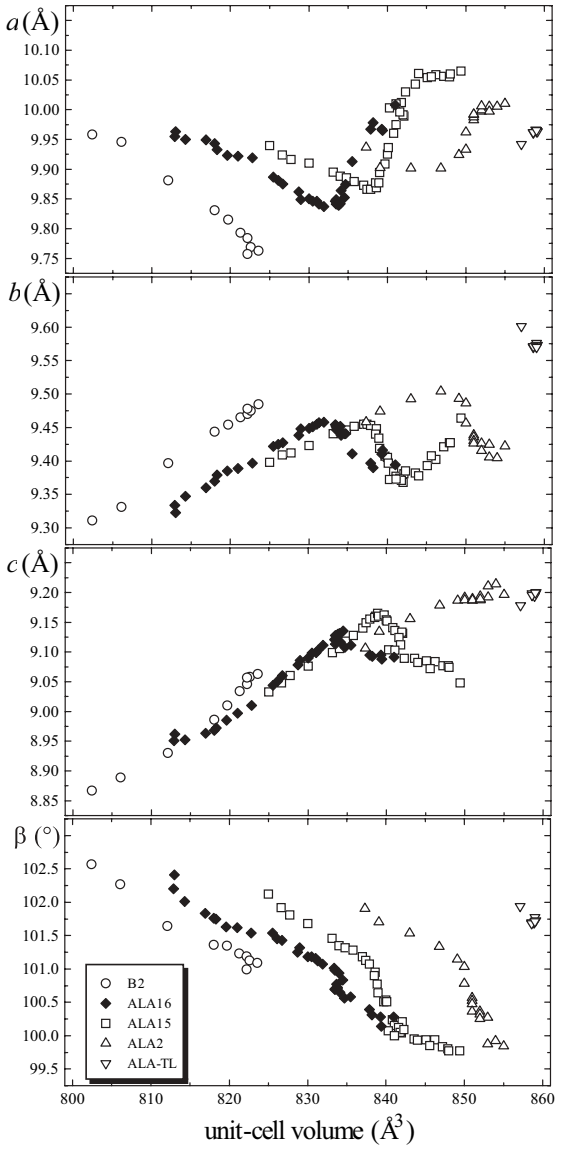

FIGURE 2. The *a*, *b*, *c* (Å), and β (°) parameters vs. the unit-cell volumes (Å^3).

TABLE 3. Fractional atomic coordinates and anisotropic displacement parameters for the arsenic sulfides at different exposure times

	x/a	*y/b*	*z/c*	U_{11}	U_{22}	U_{33}	U_{12}	U_{13}	U_{23}	U_{eq}
B2–0										
As1	–0.00187(5)	–0.20545(5)	0.05489(5)	0.0348(2)	0.0339(2)	0.0188(2)	0.0054(2)	0.0060(2)	0.0067(2)	0.0292(2)
As2	–0.16022(4)	–0.40157(5)	0.12611(5)	0.0236(2)	0.0317(2)	0.0264(2)	0.0005(2)	–0.0036(2)	–0.0065(2)	0.0286(2)
S1	0	–0.0540(2)	¼	0.0443(8)	0.0226(6)	0.0346(8)	0	0.0076(6)	0	0.0340(3)
S2	0	–0.5536(2)	¼	0.0361(8)	0.0219(6)	0.0450(9)	0	–0.0043(7)	0	0.0363(4)
S3	–0.2012(1)	–0.3040(1)	0.3403(1)	0.0262(5)	0.0493(6)	0.0318(5)	–0.0044(5)	0.0117(4)	–0.0064(5)	0.0350(3)
B2–600										
As1	0.002(2)	–0.2084(2)	0.0570(2)	0.0498(9)	0.055(1)	0.0320(7)	0.0086(8)	0.0063(5)	0.0094(7)	0.0459(6)
As1b	0.043(2)	–0.166(1)	0.095(2)	0.09(1)	0.043(7)	0.20(2)	0.027(7)	0.05(1)	0.059(9)	0.112(7)
As2	–0.1606(2)	–0.4022(2)	0.1282(2)	0.0362(8)	0.0499(9)	0.0550(9)	0.0038(6)	–0.0034(6)	–0.0137(7)	0.0488(5)
As2b	–0.120(2)	–0.459(2)	0.169(2)	0.068(8)	0.11(1)	0.082(9)	–0.033(8)	0.035(7)	–0.063(8)	0.085(6)
S1	0	–0.0590(4)	¼	0.070(2)	0.042(2)	0.073(3)	0	0.011(2)	0	0.062(1)
S2	0	–0.5525(4)	¼	0.054(3)	0.034(2)	0.098(4)	0	–0.005(2)	0	0.065(2)
S3	–0.2034(3)	–0.3065(3)	0.3385(4)	0.042(1)	0.083(2)	0.066(2)	–0.008(1)	0.023(1)	–0.011(2)	0.0622(8)
S4	–0.095(2)	–0.320(2)	–0.006(2)	0.09(1)	0.09(1)	0.044(8)	0.05(1)	0.024(9)	0.017(9)	0.076(8)
B2–840										
As1	0.0006(3)	–0.2097(4)	0.0576(2)	0.061(1)	0.076(2)	0.044(1)	0.012(1)	0.0089(8)	0.013(1)	0.0607(9)
As1b	0.046(2)	–0.166(1)	0.093(2)	0.093(9)	0.053(7)	0.21(2)	0.019(6)	0.027(9)	0.043(8)	0.121(7)
As2	–0.1606(3)	–0.4052(3)	0.1318(3)	0.043(1)	0.065(1)	0.077(1)	0.0068(9)	–0.0016(9)	–0.020(1)	0.0635(8)
As2b	–0.114(1)	–0.466(2)	0.176(1)	0.054(5)	0.101(9)	0.072(6)	–0.009(6)	0.023(4)	–0.045(6)	0.074(4)
S1	0	–0.0621(5)	¼	0.083(3)	0.053(3)	0.094(4)	0	0.017(3)	0	0.077(2)
S2	0	–0.5519(6)	¼	0.061(4)	0.047(3)	0.137(7)	0	–0.001(4)	0	0.084(3)
S3	–0.2045(4)	–0.3094(5)	0.3377(5)	0.050(2)	0.110(3)	0.084(2)	–0.004(2)	0.027(2)	–0.013(3)	0.079(1)
S4	–0.102(2)	–0.325(2)	–0.004(2)	0.09(1)	0.09(1)	0.041(7)	0.05(1)	0.004(7)	0.002(8)	0.075(7)
ALA16–0										
As1	–0.0041(2)	–0.2081(2)	0.0561(2)	0.0430(8)	0.0534(9)	0.0353(6)	0.0086(7)	0.0082(6)	0.0075(6)	0.0439(4)
As1b	0.055(2)	–0.170(2)	0.074(2)	0.068(9)	0.071(8)	0.101(9)	0.023(7)	0.014(7)	0.013(7)	0.081(4)
As2	–0.1608(1)	–0.4033(2)	0.1285(2)	0.0302(5)	0.0472(9)	0.0457(7)	0.0021(5)	–0.0019(4)	–0.0080(7)	0.0425(4)
As2b	–0.127(2)	–0.468(2)	0.176(2)	0.076(7)	0.053(7)	0.067(7)	–0.013(6)	0.022(6)	–0.006(6)	0.064(4)
S1	0	–0.0561(3)	¼	0.054(2)	0.044(2)	0.058(2)	0	0.008(2)	0	0.0522(8)
S2	0	–0.5549(4)	¼	0.044(2)	0.033(2)	0.074(3)	0	–0.005(2)	0	0.053(1)
S3	–0.2012(2)	–0.3080(3)	0.3407(3)	0.037(1)	0.078(2)	0.059(1)	–0.005(1)	0.021(1)	–0.007(1)	0.0562(7)
S4	–0.101(2)	–0.323(2)	–0.007(2)	0.06(1)	0.06(1)	0.07(1)	0.001(9)	0.024(9)	0.01(1)	0.062(6)
ALA16–1800										
As1	–0.0031(6)	–0.2134(6)	0.0591(4)	0.071(3)	0.083(3)	0.052(2)	0.012(2)	0.008(2)	0.013(2)	0.069(2)
As1b	0.056(2)	–0.169(1)	0.075(2)	0.092(8)	0.059(6)	0.16(1)	0.002(5)	0.036(7)	0.012(5)	0.104(4)
As2	–0.1618(5)	–0.4080(6)	0.1359(7)	0.059(2)	0.075(3)	0.090(3)	0.008(2)	–0.004(2)	–0.021(2)	0.077(1)
As2b	–0.119(1)	–0.465(2)	0.177(1)	0.076(7)	0.095(9)	0.068(6)	–0.014(6)	0.022(5)	–0.029(5)	0.078(4)
S1	0	–0.0621(7)	¼	0.106(5)	0.062(4)	0.097(5)	0	0.016(4)	0	0.089(2)
S2	0	–0.558(1)	¼	0.080(7)	0.047(6)	0.18(1)	0	–0.017(8)	0	0.107(5)
S3	–0.2032(5)	–0.3152(7)	0.3379(6)	0.065(3)	0.130(5)	0.093(4)	–0.009(3)	0.032(3)	–0.004(3)	0.094(2)
S4	–0.101(2)	–0.321(2)	–0.007(1)	0.11(1)	0.10(1)	0.040(7)	0.03(1)	–0.003(7)	–0.006(7)	0.084(7)
ALA15–600										
As1	–0.0065(8)	–0.217(1)	0.0577(8)	0.077(4)	0.082(5)	0.051(3)	0.004(3)	0.006(3)	0.009(3)	0.071(2)
As1b	0.049(2)	–0.172(1)	0.074(2)	0.10(1)	0.055(7)	0.110(9)	0.019(5)	0.015(7)	0.010(6)	0.090(4)
As2	–0.1633(7)	–0.4085(8)	0.136(1)	0.054(3)	0.069(4)	0.096(5)	0.008(2)	–0.006(3)	–0.021(3)	0.076(2)
As2b	–0.121(2)	–0.463(2)	0.176(2)	0.080(9)	0.094(9)	0.072(7)	–0.018(6)	0.032(6)	–0.035(6)	0.080(5)
S1	0	–0.0629(9)	¼	0.101(6)	0.060(5)	0.109(7)	0	0.027(6)	0	0.089(3)
S2	0	–0.560(1)	¼	0.056(8)	0.052(8)	0.19(2)	0	–0.03(1)	0	0.107(7)
S3	–0.2032(6)	–0.3167(7)	0.3381(8)	0.065(3)	0.116(5)	0.093(5)	–0.015(3)	0.032(3)	–0.005(4)	0.089(2)
S4	–0.104(2)	–0.324(2)	–0.008(2)	0.12(1)	0.07(1)	0.06(1)	0.03(1)	–0.01(1)	–0.004(9)	0.087(7)

DISCUSSION

The structural models obtained for B2-600, B2-840, ALA15-600, ALA16-0, and ALA16-1800 are consistent with the coexistence in the structure of two kinds of cage-like molecules. The first one (2As1 + 2As2 + S1 + S2 + 2S3) is identical to the As_4S_4 molecule found in the structures of both realgar and β-phase (Mullen and Nowacki 1972; Porter and Sheldrick 1972), in that each As atom links one As and two S atoms (Fig. 3a). The other molecule (2As1b + 2As2b + S1 + 2S3 + 2S4) is chemically and structurally identical to the As_4S_5 (Fig. 3b) found in alacranite (Bonazzi et al. 2003a), uzonite (Bindi et al. 2003), and wakabayashilite (Bonazzi et al. 2005). It can be derived from the As_4S_4 molecule by removing S2 (4*e* Wyckoff position) and adding two S4 atoms (8*f* Wyckoff position). The intramolecular distances, reported in Table 4, are consistent with those previously observed in the other arsenic sulfides containing As_4S_4 and As_4S_5 molecules (Mullen and Nowacki 1972; Porter and Sheldrick 1972; Whitfield 1973b; Burns and Percival 2001; Bonazzi et al. 2003a, 2003b; Bindi et al. 2003). Nonetheless, the As1b-S1, As1b-S3, and As2b-S3 distances slightly deviate from the expected values. This is reasonable because S1 and S3 are average positions for both As_4S_4 and As_4S_5 molecules; an attempt to refine the split positions S1-S1b and S3-S3b, however, was not successful.

The results of the structure refinements clearly show that the percentage of the As_4S_5 molecule in the structure increases when

a crystal is exposed to light. In Figure 4 the unit-cell volume is plotted as a function of the percentage of the As_4S_5 molecule obtained from the structure refinements together with the regression line $V = 801(2) + 1.04(5)$ [% As_4S_5] (Å^3) ($r = 0.989$) obtained by Bonazzi et al. (2003b) for the As_8S_{9-x} crystals from Kateřina Mine and data from literature. The behavior of the light-exposed crystals is similar to that of the non-stoichiometric As_8S_{9-x} sulfides, at least as far as the volume variations are concerned. Nonetheless, the expansion of the unit cell as a function of the As_4S_5 percentage shows some differences by examining the individual lattice parameters. In the untreated As_8S_{9-x} crystals, the expansion of the unit cell occurs by a lengthening of both *b* and *c* parameters whereas *a* remains almost unchanged. Such a behavior resembles that initially induced by light exposure, although "path I" is characterized by a decrease of the *a* parameter. A tentative explanation can be formulated by invoking a different mechanism for the substitution of As_4S_5 for As_4S_4 molecules: Due to the intrinsic limit of the diffraction technique, we can only observe a disordered mixture of As_4S_4 and As_4S_5 molecules packed in the same way as in the β-As_4S_4 phase, without any indication of the long- or short-range character of the disorder observed. As far as

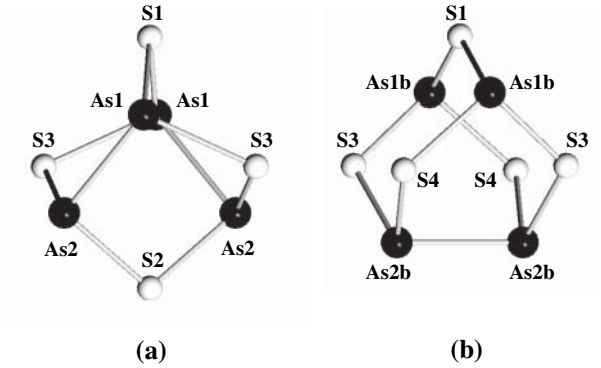

FIGURE 3. As_4S_4 (**a**) and As_4S_5 (**b**) molecules viewed along the **c** axis.

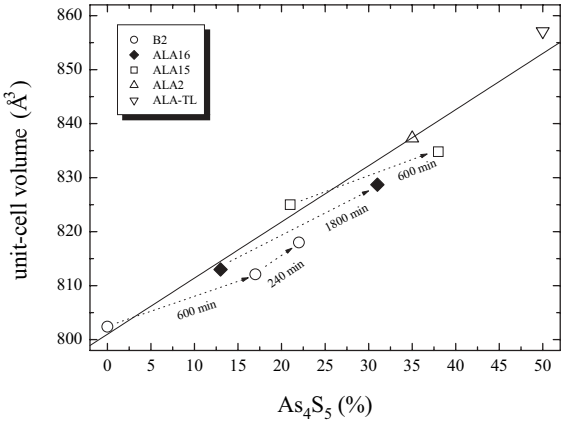

FIGURE 4. Unit-cell volumes (Å^3) plotted against the percentage of the As_4S_5 molecule obtained from structure refinements. The regression line refers to the model obtained by Bonazzi et al. (2003b).

TABLE 4. Selected interatomic distances (Å) for the arsenic sulfides after different exposure times

B2-0			B2-600			B2-840		
As_4S_4 mol.			*As_4S_4 mol.*			*As_4S_4 mol.*		
As1 -	S1	2.229(1)	As1 -	S1	2.224(3)	As1 -	S1	2.222(4)
	S3	2.231(1)		S3	2.235(3)		S3	2.246(5)
	As2	2.579(1)		As2	2.580(3)		As2	2.604(5)
As2 -	S3	2.222(1)	As2 -	S3	2.199(4)	As2 -	S3	2.178(5)
	S2	2.235(1)		S2	2.235(3)		S2	2.209(5)
	As1	2.579(1)		As1	2.580(3)		As1	2.604(5)
			As_4S_5 mol.			*As_4S_5 mol.*		
			As1b -	S3	2.06(1)	As1b -	S3	2.06(1)
				S1	1.83(2)		S1	1.85(2)
				S4	2.06(3)		S4	2.15(3)
			As2b -	S4	2.09(3)	As2b -	S4	2.12(2)
				S3	2.35(1)		S3	2.37(1)
				As2b	2.52(3)		As2b	2.37(3)
ALA15-600			**ALA16-0**			**ALA16-1800**		
As_4S_4 mol.			*As_4S_4 mol.*			*As_4S_4 mol.*		
As1 -	S1	2.272(9)	As1 -	S1	2.236(3)	As1 -	S1	2.241(6)
	S3	2.303(9)		S3	2.257(3)		S3	2.279(7)
	As2	2.57(1)		As2	2.570(3)		As2	2.59(1)
As2 -	S3	2.14(1)	As2 -	S3	2.213(3)	As2 -	S3	2.142(7)
	S2	2.25(1)		S2	2.236(3)		S2	2.230(9)
	As1	2.57(1)		As1	2.570(3)		As1	2.59(1)
As_4S_5 mol.			*As_4S_5 mol.*			*As_4S_5 mol.*		
As1b -	S3	2.09(2)	As1b -	S3	1.97(1)	As1b -	S3	2.04(1)
	S1	2.05(2)		S1	2.08(1)		S1	2.05(1)
	S4	2.11(3)		S4	2.12(3)		S4	2.14(3)
As2b -	S4	2.16(2)	As2b -	S4	2.19(2)	As2b -	S4	2.19(2)
	S3	2.29(1)		S3	2.33(1)		S3	2.30(1)
	As2b	2.51(3)		As2b	2.60(3)		As2b	2.46(3)

the untreated As_8S_{9-x} crystals are concerned, it was hypothesized that they consist of a simultaneous presence of β-As_4S_4 (*C*2/*c*) and As_8S_9 (*P*2/*c*) microdomains (Bonazzi et al. 2003a), which accounts for the gradual change of the translation symmetry (from *C* to *P*) observed from the β-phase to alacranite. On the contrary, in the case of the light-altered crystals, the intensity of the reflections violating the *C* symmetry does not increase as a function of the As_4S_5 content. Therefore, one can conclude that the relative increase of As_4S_5 molecules in the structure occurs by a random replacement of As_4S_5 for As_4S_4 without any change in the size or in the number of alacranite microdomains. In other words, the light-induced reaction $5As_4S_4 + 3O_2 \rightarrow 4As_4S_5 + 2As_2O_3$ may not produce an ordered sequence of As_4S_4 and As_4S_5 molecules as in the structure of stoichiometric alacranite. Because no evidence of arsenolite was found by X-ray diffraction experiments, it could be assumed that the As lost during alteration forms tiny, randomly oriented arsenolite crystallites or, more likely, an amorphous phase.

Differences in the ordering of As_4S_4 and As_4S_5 molecules could be a sensible reason for the slight differences observed in the variation of lattice parameters during "path I" with respect to the trends observed along the As_4S_4 – As_8S_9 join. It is a fact, however, that structural data obtained for light-exposed crystals definitively confirm that at this stage the molecule As_4S_4 is able to incorporate sulfur to transform into As_4S_5 upon exposure to light.

On the other hand, owing to the extremely low diffraction quality of the crystals during "path II" and "path III," no structural analysis was possible. Therefore, we cannot understand what happens during the last part of the alteration process. In principle, other reactions could take place to account for the increase of the unit-cell volume, such as a transformation of As_4S_5 into As_4S_6. Nonetheless, the light-exposure experiments previously carried out on compounds containing the As_4S_5 molecule (Bindi et al. 2003; Bonazzi et al. 2005) confirmed the high stability of the As_4S_5 molecule. Thus, the reason of the inversion from "path I" to "path II" has to be found in a change of mechanism which, however, still involves the addition of sulfur to the As_4S_4 molecule.

All the As_4S_n molecules can be described as $As_4S_n\bigtriangledown_{6-n}$ (n = 3, 4, and 5) groups, with As atoms located at the vertices of a disphenoid (more or less regular) and S atoms bridging n among the six available (As-As) edges. There are (6-n) disphenoidic edges corresponding to As-As bonds, while the others n correspond to longer non-bonded As-As distances. With the increase of the S content at two positions [S4 (×2) along "path I"], two corresponding As1-As2 edges increase, while the As2-As2 edge becomes shorter as the S content at the S2 position decreases. Such a variation in the geometry of the As_4 disphenoidic group, combined with the hindrance of the additional S atom and some rotation of the molecule, causes the variation of the lattice parameters observed along "path I." We could tentatively hypothesize that along "path II" the incorporation of additional sulfur occurs at the remaining, available sixth position (vacant in the original As_4S_4 molecule and throughout "path I"), thus causing lengthening of the As1-As1 edge, shortening of one of the other five As-As edges, and different rotations of the molecule producing opposite effects on lattice parameters. Likewise, other inversions ("path III") observed in the trend of lattice parameters (Fig. 2) might be related to further changes in the position of additional or lacking sulfur atoms.

Our experiments confirmed that the As_4S_4 molecule is able to incorporate sulfur to transform into As_4S_5 upon exposure to light, whereas both As_4S_3 and As_4S_5 molecules do not undergo any modification. However, the results obtained up to now suggested that the extent of sulfur incorporation is strictly controlled by the type of the molecular packing, not only by the kind of molecule.

The first fact to note is that in light-exposed single crystals of realgar (α-As_4S_4), which contain the same kind of molecule as β-As_4S_4, the increase in unit-cell volume [~1.6–1.8% and ~1.4% as reported by Bonazzi et al. (1996) and Kyono et al. (2005), respectively] is much less than that observed for the β-phase (2.6%). The small increase of the volume of the realgar unit cell probably corresponds to a limited, undetectable conversion of As_4S_4 to As_4S_5 or, alternatively, to As_4S_4 molecules of the type found in pararealgar (Ballirano et al. 2005), which show a larger molecular volume. According to the model elaborated by Kyono et al. (2005), additional sulfur would be incorporated to produce As_4S_5 molecules, and then released by breaking an equivalent As-S-As linkage to form As_4S_4 molecules of pararealgar. The process could cyclically continue by re-attachment of the free S to another As_4S_4 (realgar-type). In spite of the ingenuity of the model, however, no structural evidence for the change of S positions resulted from their structural data and, in the opinion of Kyono et al. (2005), the continuous increase of the unit-cell volume observed for realgar is to be ascribed only to the variation of the intermolecular distances.

The second fact to note is that the unit-cell expansion for the crystal of stoichiometric alacranite is negligible when compared with that of the other crystals [ΔV = 2.6 (B2), 3.2 (ALA16), 2.9 (ALA15), 1.9 (ALA2), and 0.2% (ALA-TL)]. This indicates that the As_4S_4 molecule contained in the *P*2/*c* structure of alacranite is unable to incorporate sulfur. Therefore one can speculate that in the intermediate As_8S_{9-x} phases only the β-As_4S_4 (*C*2/*c*) microdomains are involved in the alteration process, while the alacranite microdomains maintain their ordered *P*2/*c* structure with As_4S_4:As_4S_5 = 1:1. This is consistent with the observation that the β-As_4S_4 crystal completely converts to pararealgar, whereas decreasing amounts of pararealgar were observed in ALA16 and ALA15, respectively. ALA2 crystal, which contained a minor number of β-As_4S_4 (*C*2/*c*) microdomains before light exposure, produces an undetectable amount of pararealgar. It is not easy to verify when the β-As_4S_4 (*C*2/*c*) → pararealgar (*P*2$_1$/*c*) conversion starts, although it could be hypothesized that the break in slope observed in the increase of unit-cell volume vs. exposure time (Fig. 1) may be related to an incipient conversion of a part of As_4S_5 molecules into As_4S_4 (pararealgar type) molecules. It should be noted that packing of As_4S_4 molecules in the structure of β-As_4S_4 is nearly identical to that of As_4S_4 molecules (pararealgar type) in the structure of pararealgar (Fig. 5). Therefore, the transformation of β-As_4S_4 into pararealgar does not require a complete rearrangement of the molecular packing. On the other hand, transformation of realgar into pararealgar occurs through the formation of an intermediate product—the so-called χ phase first described by Douglass et al. (1992)—which has now been

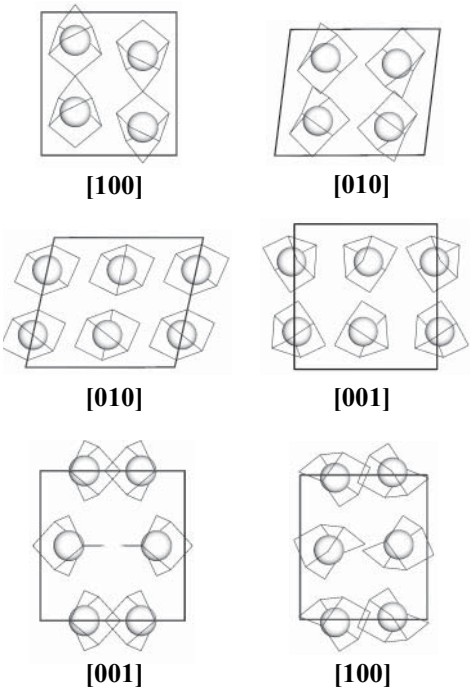

FIGURE 5. Molecular packing in the structure of β-As_4S_4 (left) and pararealgar (right). Gray circles represent the centroid of the As_4 groups; black sticks indicate the As-S and As-As bonds within the cage-like molecules.

proven definitively to consist of a β-As_4S_4 structure (*C*2/*c*) with As_4S_5 molecules randomly substituting for As_4S_4. Therefore, the alteration of realgar into pararealgar requires a complete rearrangement of the molecular packing and cannot be followed step by step by single-crystal diffraction investigation.

ACKNOWLEDGMENTS

The authors thank Daniele Borrini (Dipartimento di Scienze della Terra, Università di Firenze) for his help in the synthesis of β-As_4S_3. The paper benefited from constructive reviews by Richard Thompson and an anonymous referee. This work was funded by C.N.R. (Istituto di Geoscienze e Georisorse, sezione di Firenze) and by M.I.U.R., project P.R.I.N.-2003 "Structural complexity in minerals: modulation and modularity."

REFERENCES CITED

Ballirano, P. and Maras, A. (2002) Preliminary results on the light-induced alteration of realgar: kinetics of the process. Plinius, 28, 35–36.

Ballirano, P., Boiocchi, M., Callegari, A., and Maras, A. (2005) Single-crystal light-induced alteration of realgar: preliminary data. 5th Forum Italiano di Scienze della Terra-Geoitalia 2005, Abstract Volume, p. 238.

Bindi, L., Popova, V.I., and Bonazzi, P. (2003) Uzonite, As_4S_5, from the type-locality: X-ray single-crystal study and lighting experiments. Canadian Mineralogist, 41, 1463–1468.

Bonazzi, P., Menchetti, S., and Pratesi, G. (1995) The crystal structure of pararealgar, As_4S_4. American Mineralogist, 80, 400–403.

Bonazzi, P., Muniz-Miranda, M., and Sbrana, G. (1996) Light-induced variations in realgar and β-As_4S_4: X-ray diffraction and Raman studies. American Mineralogist, 81, 874–880.

Bonazzi, P., Bindi, L., Olmi, F., and Menchetti, S. (2003a) How many alacranites do exist? A structural study of non-stoichiometric As_8S_{9-x} crystals. European Journal of Mineralogy, 15, 282–288.

Bonazzi, P., Popova, V.I., Pratesi, G., and Menchetti, S. (2003b) Alacranite, As_8S_9: structural study of the holotype and re-assignment of the original chemical formula. American Mineralogist, 88, 1796–1800.

Bonazzi, P., Lampronti, G.I., Bindi, L., and Zanardi, S. (2005) Wakabayashilite, $[(As, Sb)_6S_9][As_4S_5]$: crystal structure, pseudosymmetry, twinning, and revised chemical formula. American Mineralogist, 90, 1108–1114.

Burns, P.C. and Percival, J.B. (2001) Alacranite, As_4S_4: a new occurrence, new formula, and determination of the crystal structure. Canadian Mineralogist, 39, 809–818.

Douglass, D.L., Shing, C., and Wang, G. (1992) The light-induced alteration of realgar to pararealgar. American Mineralogist, 77, 1266–1274.

Hall, H.T. (1966) The system Ag-Sb-S, Ag-As-S, and Ag-Bi-S: Phase relations and mineralogical significance. Ph.D. thesis, Brown University, Providence, Rhode Island.

Kutoglu, A. (1976) Darstellung und Kristallstruktur einer neuen isomeren Form von As_4S_4. Zeitschrift für anorganische und allgemeine Chemie, 419, 176–184.

Kyono, A., Kimata, M., and Hatta, T. (2005) Light-induced degradation dynamics in realgar: in situ structural investigation using single-crystal X-ray diffraction study and X-ray photoelectron spectroscopy. American Mineralogist, 90, 1563–1570.

Mullen, D.J.E. and Nowacki, W. (1972) Refinement of the crystal structures of realgar, AsS and orpiment, As_2S_3. Zeitschrift für Kristallographie, 136, 48–65.

Muniz-Miranda, M., Sbrana, G., Bonazzi, P., Menchetti, S., and Pratesi, G. (1996) Spectroscopic investigation and normal mode analysis of As_4S_4 polymorphs. Spectrochimica Acta, A52, 1391–1401.

North, A.C.T., Phillips, D.C., and Mathews, F.S. (1968) A semiempirical method of absorption correction. Acta Crystallographica, A24, 351–359.

Porter, E.J. and Sheldrick, G.M. (1972) Crystal structure of a new crystalline modification of tetra-arsenic tetrasulphide (2,4,6,8-tetrathia-1,3,5,7-tetraarsatricyclo[3,3,0,03,7]-octane). Journal of Chemical Society, Dalton Transactions, 13, 1347–1349.

Roberts, A.C., Ansell, H.G., and Bonardi, M. (1980) Pararealgar, a new polymorph of AsS, from British Columbia. Canadian Mineralogist, 18, 525–527.

Sheldrick, G.M. (1997) SHELXL-97. A program for crystal structure refinement. University of Göttingen, Germany.

Strunz, H. and Nickel, E.H. (2001) Strunz Mineralogical Tables. Chemical-Structural Mineral Classification System (9th edition). Schweizerbart, Stuttgart, Germany

Whitfield, H.J. (1970) The crystal structure of tetra-arsenic trisulphide. Journal of Chemical Society, Dalton Transactions, A, 1800–1803.

——— (1973a) Crystal structure of the β-form of tetra-arsenic trisulphide. Journal of Chemical Society, Dalton Transactions, 1737–1738.

——— (1973b) Crystal and molecular structure of tetra-arsenic pentasulphide. Journal of Chemical Society, Dalton Transactions, 1740–1742.

MANUSCRIPT RECEIVED NOVEMBER 23, 2005
MANUSCRIPT ACCEPTED APRIL 5, 2006
MANUSCRIPT HANDLED BY PRZEMYSLAW DERA